Macromolecules **2000,** *33,* 2967−2973

Effect of Core Structure on Photophysical and Hydrodynamic Properties of Porphyrin Dendrimers

M. S. Matos,[†,‡] J. Hofkens,[‡] W. Verheijen,[‡] F. C. De Schryver,*[,‡,§] S. Hecht,[||] K. W. Pollak,[||] J. M. J. Fréchet,*[,||,⊥] B. Forier,[‡] and W. Dehaen[‡]

Department of Chemistry, Katholieke Universiteit Leuven, Celestijnenlaan 200 F,
3001 Leuven (Heverlee), Belgium; and Department of Chemistry, University of California,
Berkeley, California 94720-1460

Received October 25, 1999; Revised Manuscript Received February 7, 2000

ABSTRACT: The photophysical and hydrodynamic properties of dendrimers (G*n*PZn and G*n*TPPH$_2$) with zinc porphyrin (PZn) and tetraphenylporphyrin (TPP) cores are studied in tetrahydrofuran (THF) and dimethylformamide (DMF). UV−vis absorption spectra of G*n*PZn exhibit a small red shift of the Soret band upon increasing the generation as a result of interactions between the dendrons and the core. All fluorescence decays obtained from global analysis show a monoexponential profile. The intrinsic viscosity obtained for G*n*PZn from the hydrodynamic volume (V_h) passes through a maximum as a function of generation (G) in agreement with earlier experimental findings and calculations suggesting that the internal density profile of dendrimers decrease monotonically outward from the center of the molecule. Within the investigated range ($G = 1-3$), G*n*TPPH$_2$ exhibits an approximately constant intrinsic viscosity due to the linear dependence between the hydrodynamic volume and the molecular weight. The differences observed between G*n*PZn and G*n*TPPH$_2$ are correlated to structural differences in their cores. The additional phenyl group of the TPP in G*n*TPPH$_2$ increases the distance between the branches and the porphyrin moiety compared to G*n*PZn, resulting in a more flexible structure. The enhanced flexibility allows the terminal groups to sample more conformational space and therefore decreases the volume of the dendrimer as compared to the theoretical fully extended structure where $V_h \propto G^3$. A comparison of the results obtained from analysis of fluorescence anisotropy decays with previously reported viscometry measurements shows a dependence of the structural collapse on the core size.

1. Introduction

Dendrimers are well-defined, highly branched, monodisperse macromolecules with uniform molecular weight and nanoscopic size. This class of compounds has received increasing attention during the last years due to their unique physical and chemical properties.[1−3] Recently, porphyrin-core dendrimers have been synthesized by attaching convergent Fréchet-type dendrons[4] to a porphyrin core.[5−8] Because of their large size and the possibility of host−guest interactions the porphyrins represent attractive cores for the design of dendritic sensors and catalysts. Porphyrins and metalloporphyrins are useful photophysical probes for evaluating properties of the dendritic structure due to their sensitivity to the type and position of the substitution as well as the presence of neighboring chromophores.[12] Several studies investigating dendrimers having a porphyrin or metalloporphyrin core functionality have been reported.[5,7,9−11] Nevertheless, no study has been undertaken to correlate the molecular structure of such compounds with their hydrodynamic and photophysical properties in solution. We have demonstrated the possibility to determine molecular properties from the hydrodynamic volume (V_h) at very low concentrations of the dendrimer.[13] The values of V_h are estimated via the Stokes−Einstein−Debye relation using values of rotational correlation times (ϕ) obtained from time-dependent fluorescence anisotropy experiments.

Following Tomalia's early studies,[14,15] theoretical models have been proposed to account for the properties of dendritic architectures. Murat and Grest[16] as well as Boris and Rubinstein[17] have shown the internal density profile to decrease monotonically from the center of the molecule in agreement with earlier results obtained by Lescanec and Muthukumar.[18] These theoretical predictions of a maximum of the intrinsic viscosity upon increasing the generation were experimentally supported by Mourey et al.[19]

The correlation between hydrodynamic and photophysical properties offers the opportunity to gain further insight into the dendritic structure and its dependence on the nature of the core and dendrons as well as the solvent. Using the hydrodynamic volume properties such as the intrinsic viscosity can be estimated. In this paper, we study the effects of generation number and solvent on the photophysical and hydrodynamic properties of dendrimers (G*n*PZn ($n = 1-4$) and G*n*TPPH$_2$ ($n = 1-3$), n = number of aryl ether layers) having zinc porphyrin (PZn) or free base tetraphenylporphyrin (TPP) cores covalently attached to four dendrons (Figure 1).

2. Materials and Methods

2.1. Materials. The synthesis of G*n*PZn dendrimers has been described previously.[7] All solvents used were of spectroscopic grade and stored over 4 Å molecular sieves. The optical density of the investigated solutions was always less than 0.1 to avoid spectral distortion due to the inner-filter effect. Time-resolved fluorescence measurements were performed on samples degassed by several freeze−pump−thaw cycles.

2.2. Synthesis of G*n*TPPH$_2$ (n = 1, 2, 3): General Procedure. A mixture of 5,10,15,20-tetrakis(4-hydroxyphenyl)porphyrin (69.7 mg, 0.1 mmol), [G*n*]−Br (0.5 mmol),

---

[†] Current address: Instituto de Química de São Carlos, Universidade de São Paulo, 13560-970, São Carlos-SP, Brazil.

[‡] Katholieke Universiteit Leuven.

[§] frans.deschryver@chem.kuleuven.ac.be

[||] University of California, Berkeley.

[⊥] Frechet@CChem.Berkeley.edu.

10.1021/ma991786s CCC: $19.00

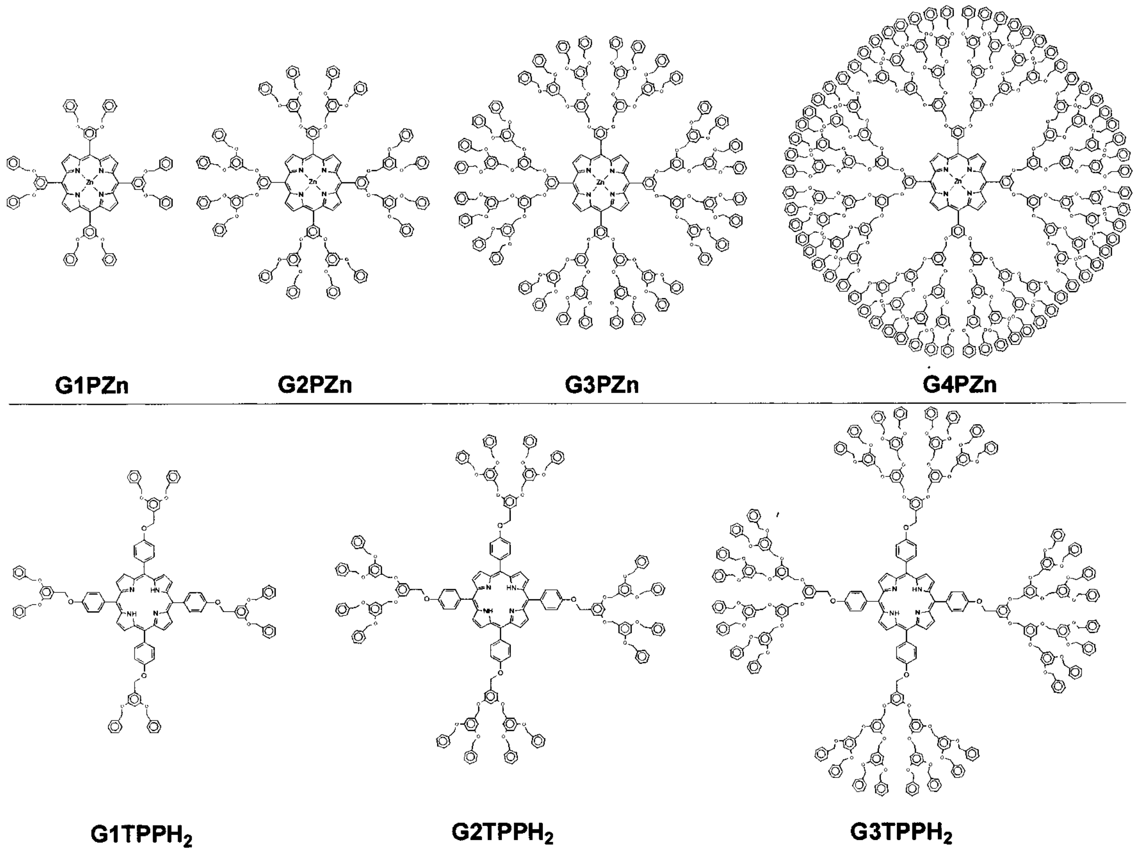

Figure 1. Representation of the two investigated dendrimers series G*n*PZn and G*n*TPPH$_2$.

K_2CO_3 (69 mg, 0.5 mmol), and 18-crown-6 (50 mg, 0.2 mmol) was refluxed in dry acetone (20 mL) during 48 h under a nitrogen blanket. After aqueous workup (100 mL), the mixture was extracted with dichloromethane (3 × 50 mL), and the organic layers were dried ($MgSO_4$) and evaporated. The residue was chromatographed on silica gel with dichloromethane as the eluent to afford the porphyrin dendrimer.

G1TPPH$_2$: 71% yield; mp 159−162 °C (chloroform/ether); ^{1}H NMR (400 MHz, $CDCl_3$, ppm) δ −2.74 (s, 2H, NH), 5.11 (s, 16H, CH_2O), 5.23 (s, 8H, CH_2O), 6.68 (t, $J = 2$ Hz, 4H, C_6H_3), 6.87 (d, $J = 2$ Hz, 8H, C_6H_3), 7.30−7.46 (m, 48H, phenyl + phenylene), 8.08 (d, $J = 8.4$ Hz, 8H, phenylene), 8.85 (s, 8H, porphyrin b H); ^{13}C NMR (100 MHz, $CDCl_3$, ppm) δ 70.2 (CH_2O), 101.7 (C_6H_3 CH-4), 106.6 (C_6H_3 CH-2,6), 113.1 (phenylene CH-3,5), 119.7 (porphyrin C-5,10,15,20), 127.6, 128.1, and 128.6 (phenyl CH), 131.0 (porphyrin CH, broad), 134.9 (phenylene C-1), 135.6 (phenylene CH-2,6), 136.8 (phenyl C), 139.5 (C_6H_3 C-1), 158.5 (phenylene C-4), 160.3 (C_6H_3 C-3,5); MS (ES+, *m*/*z*) 1888.

G2TPPH$_2$ was prepared in the same manner as a glass in 71% yield: ^{1}H NMR (400 MHz, $CDCl_3$, ppm) δ −2.75 (s, 2H, NH), 5.03 (s, 32H, CH_2O), 5.05 (s, 16H, CH_2O), 5.25 (s, 8H, CH_2O), 6.58 (t, 8H, 2nd generation Ar H-4, $J = 2$ Hz), 6.63 (t, 4H, 1st generation Ar H-4, $J = 2$ Hz), 6.73 (d, 16H, 2nd generation Ar H-2,6, $J = 2$ Hz), 6.86 (d, 8H, 1st generation Ar H-2,6, $J = 2$ Hz), 7.23−7.40 (m, 88H, phenyl and phenylene H-2,6), 8.10 (d, $J = 8.3$ Hz, 8H, phenylene H-3,5), and 8.86 (s, 8H, porphyrin b H); ^{13}C NMR (100 MHz, $CDCl_3$, ppm) δ 70.1, 70.2, and 70.3 (CH_2O), 101.6, 106.4, 139.5, and 160.3 (1st generation Ar CH-4, CH-2,6, C-1 and C-3,5), 101.7, 106.6, 139.3, and 160.2 (2nd generation Ar CH-4, CH-2,6, C-1 and C-3,5), 127.5, 128.0, 128.6, and 136.7 (phenyl CH-3,5, CH-4, CH-2,6 and C-1), 113.1, 135.0, 135.6, and 158.6 (phenylene CH-3,5, C-1, CH-2,6 and C-4), 119.7 (porphyrin C-5,10,15,20); MS (ES+, $AcONH_4$, *m*/*z*) 3586.

G3TPPH$_2$ was prepared in the same manner as a glass in 77% yield: ^{1}H NMR (400 MHz, $CDCl_3$, ppm) δ −2.75 (s, 2H, NH), 4.95 (s, 96H, CH_2O), 5.02 (s, 16H, CH_2O), 5.22 (s, 8H, CH_2O), 6.52 (t, 16H, 3rd generation Ar H-4, $J = 2.2$ Hz), 6.55 (t, 8H, 2nd generation Ar H-4, $J = 2.1$ Hz), 6.62 (t, 4H, 1st generation Ar H-4, $J = 2.0$ Hz), 6.65 (d, 32H, 3rd generation Ar H-2,6, $J = 2.2$ Hz), 6.71 (d, 16H, 2nd generation Ar H-2,6, $J = 2.1$ Hz), 6.87 (d, 8H, 1st generation Ar H-2,6, $J = 2.0$ Hz), 7.21−7.38 (m, 168H, Ph, phenylene H-3,5), 8.08 (d, 8H, C_6H_4 H-2,6, $J = 8.4$ Hz), 8.84 (s, 8H, porphyrin b H); ^{13}C NMR (100 MHz, $CDCl_3$, ppm) δ 70 (two signals, CH_2O), 101.6 (C_6H_3, CH-2,6), 106.3 and 106.5 (C_6H_3, CH-4,6), 113.1 (phenylene C-3,5), 119.7 (porphyrin C-5,10,15,20), 127.5, 127.9, 128.5, and 136.7 (phenyl CH3,5, CH-4, CH2,6 and C-1), 134.9 (phenylene C-1), 135.6 (phenylene C-2,6), 139.2 and 139.5 (C_6H_3 C-1), 160.07, 160.12, and 160.19 (C_6H_3 C-1 and C-3).

2.3. Instrumentation. The absorption spectra were measured at 20 ± 1 °C with a Perkin-Elmer Lambda 6 UV−visible spectrophotometer. Steady-state fluorescence spectra at room temperature were measured with a SPEX Fluorolog 212. The polarized emission decays were obtained by a single-photon timing technique.[20] The compounds were excited at 425 nm (for G*n*PZn) and at 420 nm (for G*n*TPPH$_2$) using the output of a titanium-sapphire laser pumped by a beam-locked argon ion laser with repetition frequency of the excitation pulses of 400 kHz. TBO (bis[1-octadecyl-benzoxazol-2-]trimethine perchlorate) in methanol ($\tau = 0.14$ ns) and coumarin 153 in ethanol ($\tau = 4.6$ ns) were used as reference compounds. The number of counts in the peak channel was approximately 10^4. Time increments of 45 and 20 ps/channel were used. The decay traces were collected at three different orientations of the emission polarizer (0°, 54.7° and 90°). The decay parameters were recovered using a global analysis-fitting program. The quantum yield of all compounds was determined from the equation

$$\Phi = \left(\frac{F_{\text{sample}}}{F_{\text{ref}}}\right)\left(\frac{A_{\text{ref}}}{A_{\text{sample}}}\right)\Phi_{\text{ref}}\left(\frac{{n_{\text{sample}}}^2}{{n_{\text{ref}}}^2}\right) \qquad (1)$$

where F_{sample} and F_{ref} are the measured fluorescence (area under the fluorescence spectra) of the sample and the reference respectively, A_{sample} and A_{ref} are the absorbances of the sample

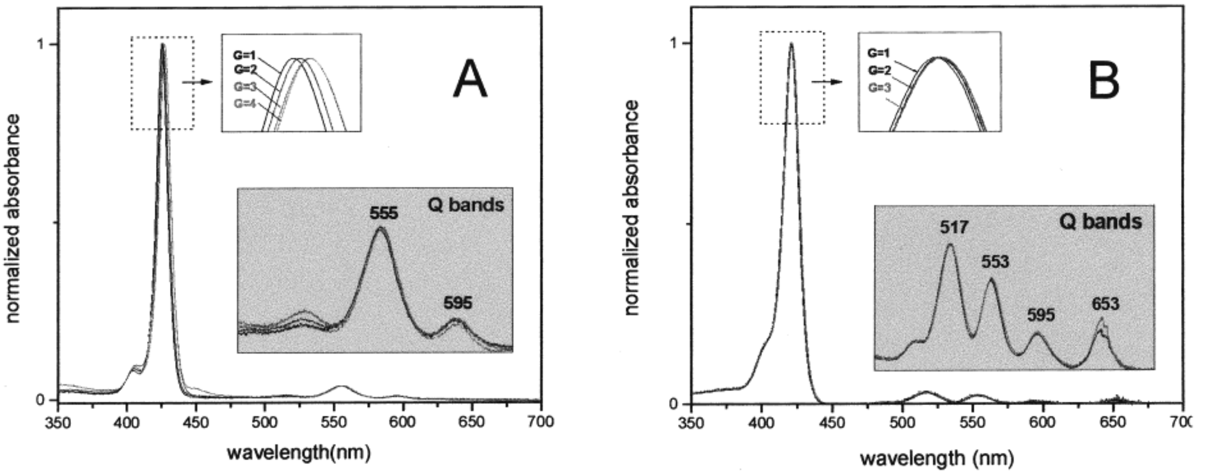

Figure 2. Absorption spectra of (A) G*n*PZn and (B) G*n*TPPH$_2$ for different generations in THF. The spectra are normalized relative to the absorption maxima.

and the reference respectively at the same excitation wavelength, Φ_{ref} is the quantum yield of the reference, and *n* is the refractive index. Tetraphenylporphyrin (TPP) in propanol was used as reference ($\Phi_f = 0.075$)[21] in our measurements.

2.4. Data Analysis. The analysis of the fluorescence decays for G*n*PZn and G*n*TPPH$_2$ was carried out at a detection wavelength of 600 nm to eliminate any contribution from traces of free base porphyrin in the zinc series (G*n*PZn). The fluorescence intensity decays, $i(\theta,\tau)$, were simultaneously analyzed using a global analysis-fitting program according to

$$I(\theta,\tau) = [\kappa(\theta)/3]\alpha \exp(-t/\tau)[1 + (3\cos^2\theta - 1)\sum_{J=1}^{m} \beta_1 \exp(-t/\phi_j)] \quad (2)$$

where *t* represents the fluorescence decay time and ϕ_j the rotational correlation times of the fluorophore. $\kappa(\theta)$ is a generally time-independent matching factor. β is a preexponential factor, which is characteristic for the fluorophore, related to the transition dipole moment of absorption and emission, and independent of the solvent. The program uses reference convolution and reference lifetime, τ_{ref}, which is in all cases freely adjustable. The equations and details of the global analysis program have been reported previously.[22] All global analyses were performed on an IBM RISC 6150−125 computer.

3. Results and Discussion

3.1. Absorption Properties. The UV−vis absorption spectra of G*n*PZn and G*n*TPPH$_2$, shown in Figure 2, are similar to the ones obtained for zinc tetraphenylporphyrin (ZnTPP) and TPP, respectively.[12] In the two different solvents, tetrahydrofuran (THF) and dimethylformamide (DMF), both Soret and Q-bands do not shift upon increasing the concentration up to 10^{-6} M, indicating the absence of intermolecular aggregation processes in the ground state. This finding was confirmed by applying a methodology developed by Pasternack et al.,[23,24] allowing the determination of porphyrin aggregates. As the generation number of G*n*PZn increases (Figure 2), a small red shift of the Soret band is observed while the Q-bands remain unchanged. In contrast, no shift is observed for G*n*TPPH$_2$. The same spectral effect was observed for similar compounds by Aida and coworkers, who suggested such a red shift to be associated with the encapsulation degree of the chromophore into the dendrimer framework.[9] In our opinion, this small red shift of the Soret band in G*n*PZn is an indication of weak interactions between the core and the branches, which could affect the photophysical properties of the porphyrin moiety.

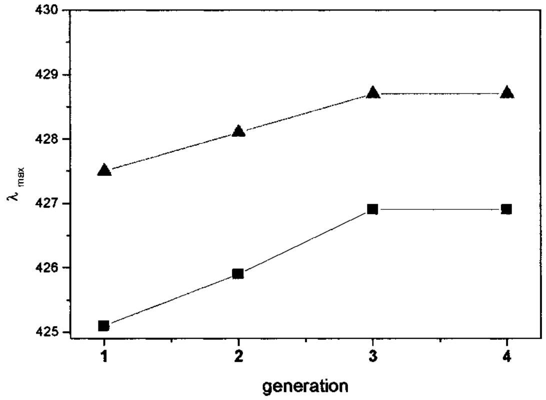

Figure 3. Dependence of the Soret band maxima on generation number for G*n*PZn in DMF (▲) and in THF (■).

As illustrated in Figure 3, the variation profile of the Soret band in G*n*PZn is similar in both solvents (THF and DMF), and the difference of energy between dendrimers of the same generation in different solvents remains approximately constant (≈0.015 eV). An analysis of the maxima of the excitation spectra in DMF and THF as a function of generation confirmed the curved profile depicted in Figure 3. These results indicate that the observed behavior is not caused by a solvent effect but rather due to enhanced interactions between the core and the dendrons as a function of generation. In addition, we suggest that the absence of a red shift starting from the third generation is caused by an increased steric crowding around the porphyrin ring disabling additional interactions between chromophore and dendrons. Physical measurements on higher generation dendrimers ($G \geq 3$) with a compact structure showing encapsulation of the core[25] support our rationalization.

3.2. Emission Properties. The emission and excitation spectra of the compounds are reported in Figure 4. A similar Stokes shift (≈10 nm) is obtained for all generations. The Q emission bands do not shift and their intensity ratio is constant for all generations in agreement with the absorption spectra where the Q-bands are unchanged. The fluorescence quantum yield (Φ_f) obtained in different solvents does not change as a

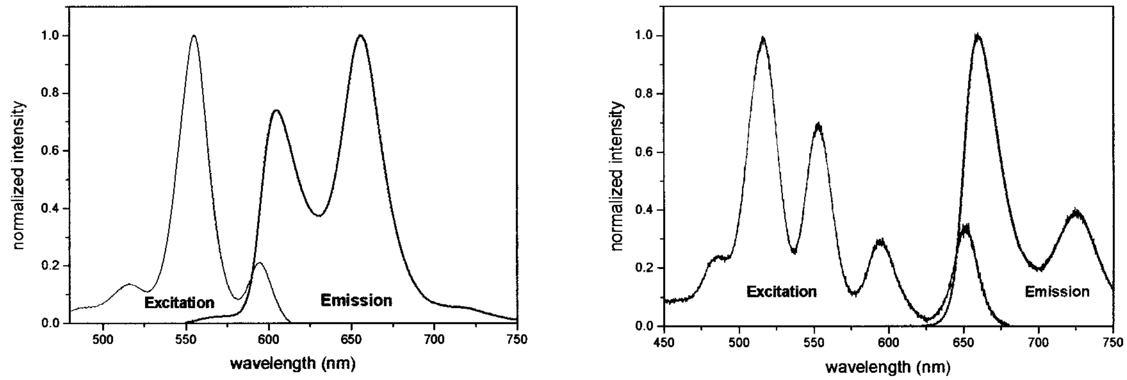

A **B**

Figure 4. Excitation and emission spectra for (A) G1Pnz and (B) G1TPPH$_2$ in THF. The spectra are normalized for comparison.

Table 1. Hydrodynamic Properties and Parameters from Global Analysis of the Fluorescence Anisotropy Decays of Porphyrin-Core Dendrimers in THF at Room Temperature, Where the Values of τ, β, and ϕ Are Freely Adjustable

compound	τ (ns)	β	ϕ (ns)	χ^2	MW	V_h (Å^3)	V_{vw} (Å^3)	V_{free} (Å^3)	ρ (g mL^{-1})	[η] (dL g^{-1})
G1TPPH$_2$	10.4	0.05	0.69	1.15	1888	4514	1660	2854	0.695	0.036
G2TPPH$_2$	10.5	0.05	1.38	1.01	3586	9051	3148	5903	0.658	0.038
G3TPPH$_2$	10.7	0.06	2.88	1.03	6982	18890	6124	12766	0.614	0.041
G1PZn	1.54	0.10	0.39	1.08	1527	2558	1293	1265	0.991	0.025
G2PZn	1.61	0.10	1.16	1.20	3221	7608	2781	4827	0.703	0.035
G3PZn	1.68	0.10	2.43	1.12	6621	15938	5757	10181	0.690	0.036
G4PZn	1.68	0.10	3.23	1.20	13413	21185	11709	9476	1.051	0.024

Table 2. Hydrodynamic Properties and Parameters from Global Analysis of the Fluorescence Anisotropy Decays of Porphyrin-Core Dendrimers in DMF at Room Temperature, Where the Values of τ, β, and ϕ Are Freely Adjustable

compound	τ (ns)	β	ϕ (ns)	χ^2	MW	V_h (Å^3)	V_{vw} (Å^3)	V_{free} (Å^3)	ρ (g mL^{-1})	[η] (dL g^{-1})
G1TPPH$_2$	10.3	0.08	0.99	1.01	1888	4041	1660	2381	0.776	0.032
G2TPPH$_2$	10.4	0.07	1.99	1.10	3586	8122	3148	4974	0.733	0.034
G3TPPH$_2$	10.3	0.07	4.29	1.07	6982	17510	6124	11386	0.662	0.038
G1PZn	1.64	0.11	0.74	1.13	1527	3020	1293	1727	0.840	0.030
G2PZn	1.72	0.12	2.13	1.12	3221	8694	2781	5913	0.615	0.041
G3PZn	1.76	0.09	3.49	1.01	6621	14245	5757	8488	0.772	0.032
G4PZn	1.77	0.09	3.63	1.03	13413	14816	11709	3107	1.503	0.017

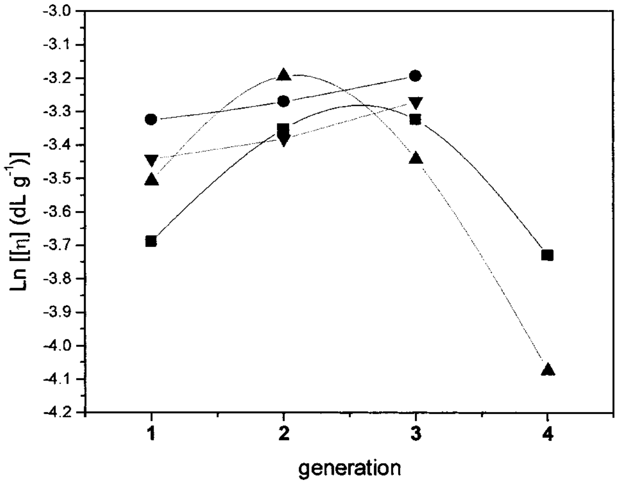

Figure 5. Logarithm of intrinsic viscosity as a function of generation number for porphyrin dendrimers: (■) G*n*PZn in THF; (▲) G*n*PZn in DMF; (●) G*n*TPPH$_2$ in THF; (▼) G*n*TPPH$_2$ in DMF.

function of generation. The Φ_f values measured for G*n*PZn and G*n*TPPH$_2$ are identical to those determined for zinc tetraphenylporphyrin ($\Phi_f = 0.033$)[26] and tetraphenylporphyrin ($\Phi_f = 0.11$),[27] respectively. This result suggests little influence of the dendrons on the nonradiative and radiative deactivation processes of the porphyrin core.

3.3. Fluorescence Depolarization and Hydrodynamic Properties. The hydrodynamic properties and the anisotropy parameters obtained from global analysis of three decays at different angles of the emission polarizer are shown in Tables 1 and 2. All fluorescence decays show a monoexponential profile in both dendrimer series. The values of the decay time (τ) do not change in G*n*PZn as well as in G*n*TPPH$_2$. The observed small variation (1.6−1.7 ns) of the decay time for G*n*PZn is within the experimental error (10%). The anisotropy decays of all generations are fitted to a single-exponential model. The β values obtained for all generations are similar to the values of the limiting anisotropy (r_0) of ZnTPP and TPP[28] ($\beta = 0.11$). In both dendritic systems, ϕ increases as the dendrimer becomes larger as predicted on the basis of the Stokes−Einstein−Debye relation

$$\phi = V_h\eta/kT \qquad (3)$$

where V_h is the hydrodynamic volume, η the viscosity of the solvent, k the Boltzmann constant, and T the absolute temperature. Structural changes are deduced from changes in the free volume, V_{free} (the difference between van der Waals volume, V_{vw} and hydrodynamic volume, V_h), where the van der Waals volumes are calculated from Edward's increments.[29] The values for V_{free} show a collapse of the structure between the third and fourth generation for G*n*PZn in both solvents in

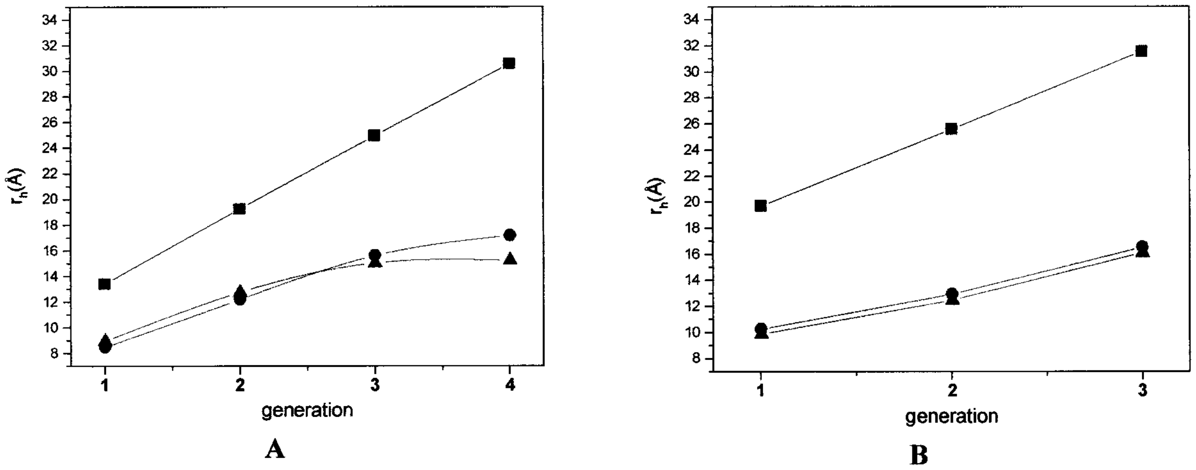

Figure 6. Hydrodynamic radius as a function of generation number for porphyrin dendrimers: (A) (■) G*n*PZn in gas phase, (●) G*n*PZn in THF, and (▲) G*n*PZn in DMF; (B) (■) L*n*TPPH$_2$ in gas phase, (●) G*n*TPPH$_2$ in THF, and (▲) G*n*TPPH$_2$ in DMF.

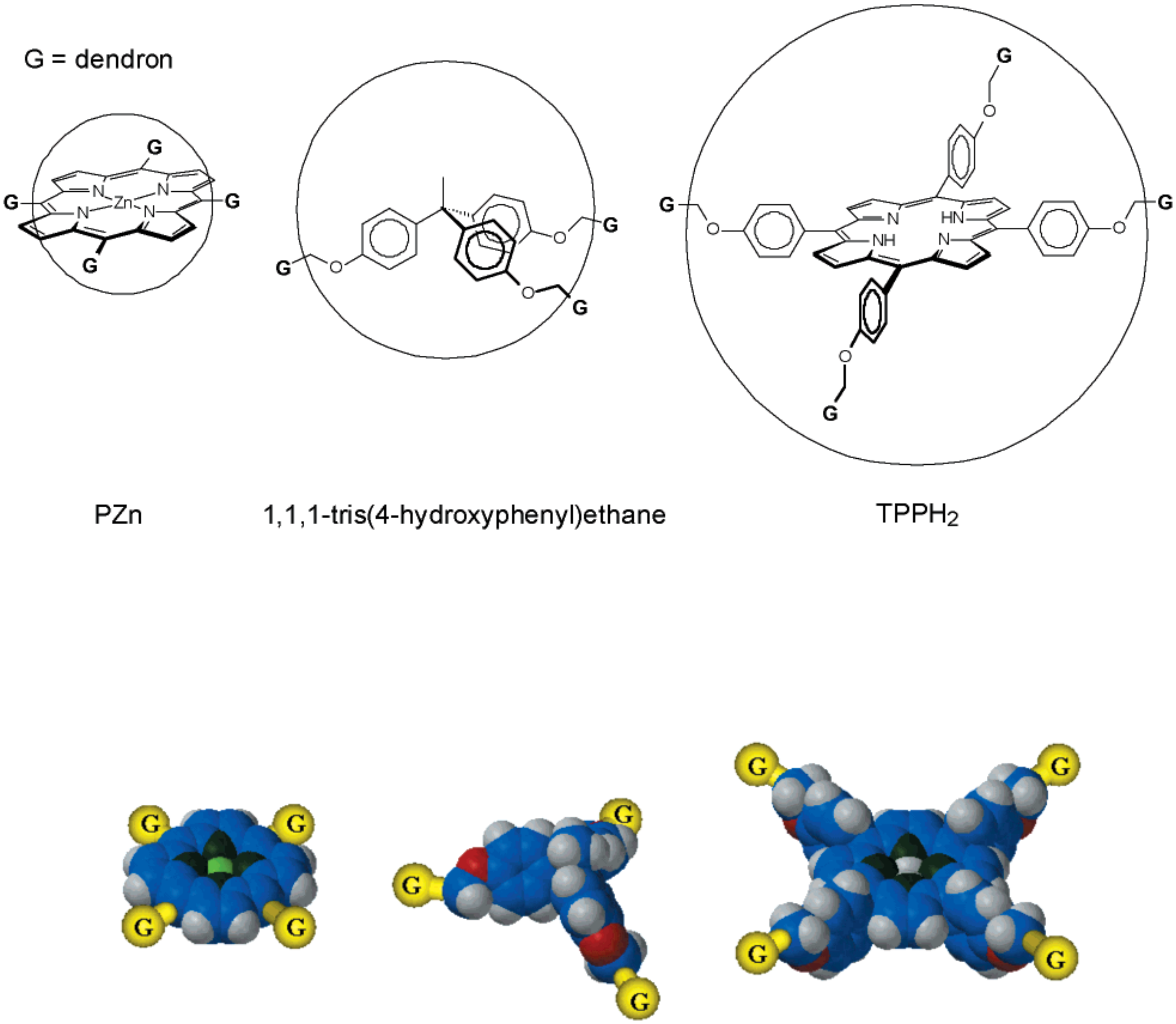

Figure 7. Structural comparison of the investigated cores and their sizes. Core geometries were optimized using the Merck force field implemented in Spartan 5.0.

contrast to G*n*TPPH$_2$, where no maximum is observed.

The intrinsic viscosity [η] of a dendrimer can be expressed through its hydrodynamic volume, V_h,[17] as

$$[\eta] = 2.5N_a(V_h/MW) \qquad (4)$$

where N_a is Avogadro's number and MW is the molecular weight.

As shown in Figure 5, the intrinsic viscosity for G*n*PZn dendrimers passes through a maximum as a function of generation number in both solvents. These results are in agreement with the predictions of Tomalia et al.[15] and the simulations of Lescanec and Muthukumar[18] that predict a maximum in intrinsic viscosity as a function of generation. In addition, the resulting curve profile (Figure 5) agrees well with that obtained experimentally by Mourey et al.[19] using similar polyether dendrimers.

In contrast to G*n*PZn, the values of intrinsic viscosity obtained for G*n*TPPH$_2$ (Figure 5) show only a small variation in both solvents. This effect is due to the linear dependence of V_h on molecular weight (MW) ($V_h \propto MW^{1.10}$ in DMF and $V_h \propto MW^{1.11}$ in THF), which is unusual for this class of dendrimers. The structures of G*n*TPPH$_2$ do not collapse within the investigated range of generations and their free volume increases linearly with generation.

The effect of the solvent on hydrodynamic radius (r_h) of G*n*PZn and G*n*TPPH$_2$ is shown in Figure 6. In both solvents the hydrodynamic radius ($r_h = V_h^{1/3}$) of G*n*PZn dendrimers up to the third generation has a similar value relative to that of the extended structure in the gas phase (where interactions among branches and solvent effects are excluded and $r_h \propto G$).[16] However, for the fourth generation (G4PZn), the structure collapses and the hydrodynamic radius decreases remarkably (a decrease of 2.9 Å in THF and of 6.0 Å in DMF). Interestingly, the structures of G*n*TPPH$_2$ are not fully extended compared to their gas-phase radii indicating a more dense structure than for G*n*PZn.

The differences observed for G*n*PZn and G*n*TPPH$_2$ can be explained considering their different molecular structure. The main structural difference arises from the core size, thus, having a profound effect on the resulting dendrimer architecture. As can be seen in Figure 7, the core in G*n*TPPH$_2$ is extended due to the insertion of an additional *para*-substituted phenyl ring separating the dendrons from the core. The larger core size of G*n*TPPH$_2$ leads to an increased distance between the dendrons minimizing steric hindrance as compared to G*n*PZn where the dendrons are linked directly to the porphyrin core. As a result, the branches in G*n*TPPH$_2$ are more flexible and able to adopt more conformations. This enhancement of flexibility results in a less extended structure compared to G*n*PZn and allowing the terminal groups to sample more conformational space. This structural effect would decrease the hydrodynamic volume of the dendrimer in comparison to theoretical, fully extended structures.

Relating the obtained results to work on similar Fréchet-type dendrimers using a different experimental setup employing size exclusion chromatography coupled to differential viscometry,[19] we conclude that given the same dendritic backbone, the point of structural collapse can be correlated to the size of the dendrimer core. Investigating 1,1,1-tris(4-hydroxyphenyl)ethane-cored dendrimers, Mourey and co-workers had found a viscosity maximum at the third generation. Consequently, we suggest that, with increasing core size, i.e., PZn smaller than 1,1,1-tris(4-hydroxyphenyl)ethane smaller than TPPH$_2$, the maximum of the intrinsic viscosity is shifted toward higher generation (Figure 7). In addition to the core size, the rigidity of the core and the number of the dendritic substituents will certainly influence the hydrodynamic properties, but such contributions cannot be deconvoluted from the current data.

4. Conclusions

Polyaryl ether dendrimers with PZn and TPP cores do not aggregate in solution and exhibit intramolecular interactions between the porphyrin unit and the dendrons in the ground state. The value of intrinsic viscosity for G*n*PZn passes through a maximum as a function of generation in qualitative agreement with other experimental[13,19] and theoretical studies.[14–18] In contrast to the zinc series, G*n*TPPH$_2$ exhibits an intrinsic viscosity approximately constant with generation in the investigated range ($n = 1-3$). The different behavior is attributed to structural differences in the two dendrimer series studied caused by an additional phenyl group further separating the dendrons and the core moiety. This extra spacer increases the distance between the dendrons minimizing steric hindrance and leading to an enhanced flexibility. Therefore, the terminal groups sample more conformational space and the hydrodynamic volume decreases compared to the theoretical fully extended structures in the gas phase. Comparison with viscosity measurements[19] that complement our experimental approach shows the important contribution of core size to the hydrodynamic properties of dendritic structures in general.

Acknowledgments. The authors thank the DWTC, through IUAP-IV-11, and ESF SMARTON for financial support. W.V. thanks the IWT for a predoctoral scholarship. J.H. is a postdoctoral fellow of the Fund for Scientific Research-Flanders. M.S.M. thanks FAPESP and KULeuven for a fellowship. Financial support from the AFOSR-MURI program and the National Science Foundation (NSF-DMR 9816166) is acknowledged with thanks.

References and Notes

(1) Tomalia, D. A. *Adv.* ***Mater.*** **1994, *6*, 529.**
(2) Fréchet, J. M. J. *Science* **1994**, *263*, 1710.
(3) Newkome, G. R.; Moorefield, C. N.; Vögtle, F. *Dendritic Molecules*; *Concepts*, *Synthesis*, *Perspectives*; VCH: Weinheim, Germany, 1996.
(4) Hawker, G. J.; Fréchet, J. M. J. *J. Am. Chem. Soc.* **1990**, *112*, 7638.
(5) Jin, R.-H.; Aida, T.; Inoue, S. *J. Chem. Soc., Chem. Commun.* **1993**, 1260.
(6) Bhyrappa, P.; Young, J. K.; Moore, J. S.; Suslick, K. S. *J. Am. Chem. Soc.* **1996**, *118*, 5708.
(7) Pollak, K. W.; Leon, J. W.; Fréchet, J. M. J.; Maskus, M.; Abruña, H. D. *Chem. Mater.* **1998**, *10*, 30.
(8) An aliphatic ester dendrimer backbone has been used by: Dandliker, P. J.; Diederich, F.; Zingg, A.; Gisselbrecht, J.-P.; Gross, M.; Louati, A.; Sanford, E. *Helv. Chim. Acta* **1997**, *80*, 1773 and references therein.
(9) Tomoyose, Y.; Jiang, D. L.; Jin, R. H.; Aida, T.; Yamashita, T.; Horic, K. *Macromolecules* **1996**, *29*, 5236.
(10) Sadamoto, R.; Tomioka, N.; Aida, T. *J. Am. Chem. Soc.* **1996**, *118*, 3978.
(11) Jiang, D.-L.; Aida, T. *J. Am. Chem. Soc.* **1998**, *120*, 10895.
(12) Dolphin, D. *The Porphyrins*; Academic Press: New York, 1978.
(13) De Backer, S.; Prinzie, Y.; Verheijen, W.; Smet, M.; Desmedt, K.; Dehaen, W.; De Schryver, F. C. *J. Phys. Chem. A* **1998**, *102*, 5451.
(14) Tomalia, D. A.; Baker, H.; Dewald, J. R.; Hall, M.; Kallos, G.; Marin, S.; Roeck, J.; Ryder, J.; Smith, P. *Polym. J. (Tokyo)* **1985**, *17*, 117.
(15) Tomalia, D. A.; Naylor, A.; Goddard, W. A. III. *Angew. Chem., Int. Ed. Engl.* **1990**, *29*, 138.
(16) Murat, M.; Grest, G. S. *Macromolecules* **1996**, *29*, 1278.
(17) Boris, D.; Rubinstein, M. *Macromolecules* **1996**, *29*, 7251.
(18) Lescanec, R. L.; Muthukumar, M. *Macromolecules* **1990**, *23*, 2280.

(19) Mourey, T. H.; Turner, S. R.; Rubinstein, M.; Fréchet, J. M. J.; Hawker, C. J.; Wooley, K. L. *Macromolecules* **1992**, *25*, 2401.

(20) Lakowiczs, J. R. *Topics in Fluorescence Spectroscopy*; Plenum Press: New York, 1991; Vol. 1.

(21) Gradyushko, A. T.; Tsvirko, M. P. *J. Am. Chem. Soc.* **1970**, *92*, 535.

(22) Crutzen, M.; Ameloot, M.; Boens, N.; Negri, R. M.; De Schryver, F. C. *J. Phys. Chem.* **1993**, *97*, 8133.

(23) Pasternack, R. F.; Bustamante, C.; Collings, P. J.; Gianetto, A.; Gibbs, E. J.*J. Am. Chem. Soc.* **1993**, *115*, 5393.

(24) Pasternack, R. F.; Schaefer, K. F.; Hambright, P. *Inorg. Chem.* **1994**, *33*, 2062.

(25) Gorman, C. B.; Parkhust, B. L.; Su, W. L.; Chen, K. Y. *J. Am. Chem. Soc.* **1997**, *119*, 1141.

(26) Strachan, J. P.; Gentemann, J. S.; Kalsbeck, W. A.; Lindsey, J. S.; Holten, D.; Bocian, D. F. *J. Am. Chem. Soc.* **1997**, *119*, 11191.

(27) Kim, J. B.; Leonard, J. J.; Longo, F. R. *J. Am. Chem. Soc.* **1972**, *94*, 3986.

(28) Maiti, N. C.; Mazumdar, S.; Periasamy, N. *J. Phys. Chem.* **1995**, *99*, 10708.

(29) Edward, J. *J. Chem. Educ.* **1970**, *47*, 261.

MA991786S